Hydrophobic interaction is the dominant mechanism of zwitterionic PFAS adsorption to carbon-based sportive materials in solution and soil

Table S1: Artificial soil pore water (SPW) composition measured by ICP-OES and used in batch sorption experiments.

Compound name	Concentration in the artificial SPW (mM)	Cation concentration (mg/L)	
Calcium sulfate-$CaSO_4$	4	Magnesium	26.4
Magnesium nitrate- $Mg(NO_3)_2$	1.8	Calcium	163.1
Potassium chloride-KCl	1.2	Potassium	50.5
Sodium chloride-NaCl	9.7	Sodium	229.0

Synthesis of graphene-based materials (GMBs)

Synthesis of graphene oxide

Graphene oxide was synthesised by the improved Hummer's method, outlined below (Marcano *et al.*, 2010). Natural graphite was ground and sieved to < 250 μm. Concentrated sulfuric acid and phosphoric acid (9:1) was combined and then cooled in freezer for 6 h. The acid mixture was added to graphite (2 g) and potassium permanganate (12 g) mixture then stirred at 55°C for 16 h. Ice was added to the reaction mixture with stirring until the light purple paste turned to a dark purple liquid. Hydrogen peroxide (approx. 3 mL) was added slowly during vigorous stirring until the reaction mixture turned a golden yellow colour. The reaction mixture was then centrifuged at 3402 RCF using a Thermo Scientific Sorvall Centrifuge (used in all further centrifugation in this study) and washed with deionised (DI) water, dilute HCl, followed by water x 2, and the solids combined to give GO as a dark brown paste.

Synthesis of graphene-iron hybrid aerogel (rGO-Fe)

The method for synthesis of GO functionalised with Fe nanoparticles was derived from Andjelkovic *et al.* (2015). Briefly, GO was added to milli-Q water (500 mL) to give a 2 mg/mL solution, which was sonicated for 30 min. The GO solution pH was adjusted to 2.5-3.0 and added to iron sulfate heptahydrate (14 g). The reaction mixture was stirred at 90 °C for 6 – 8 hours, before being washed using DI water until the supernatant went from green-tinged to clear, giving the reduced graphene-Fe (rGO-Fe) as a black suspension.

Synthesis of polyamine modified chemically reduced graphene oxide composite (rGO-N)

The chemically reduced amine functionalised GO composite was prepared following the method by Yap *et al.* (2020). Graphene oxide was added to milli-Q water (200 mL) to give a 2 mg/mL solution,

which was sonicated for 30 min. Tetraethylene pentaamine polymer hardener (1 g) was added to milli-Q water (20 mL) and stirred thoroughly, before being added to the GO solution. The solution was stirred at room temperature for 1 hour. Hydrazine (0.1 mL) was added to the reaction mixture, which was then stirred at 90 °C for 2 hours. The solid component of the reaction mixture was separated and washed with DI water x 2 to give the polyamine modified chemically reduced GO composite (rGO-N) as a black suspension.

Reduction of graphene oxide to form graphene

Graphene was synthesised by chemically reducing the previously synthesised GO using hydrazine, according to the method by Kabiri *et al.* (2020). Hydrazine was added to dispersed 2 mg/mL GO (1 µL per 3 mg of GO), heated with stirring at 80 °C for 3 hours, and the resulting solid washed with DI water (x3) to give GN as a black suspension.

Material characterisation

The structure and functional groups of each compound were confirmed using Fourier transform infrared spectroscopy (FTIR), on a Thermo-Scientific Nicolet iS20 Smart iTX spectrometer (Figure S1). The specific surface area (SSA) was determined by measuring the absorbance of the sorbents in the presence of methylene blue solution according to the method by (Kabiri *et al.*, 2014) on a Shimadzu UV-Vis spectrophotometer at 650 nm. The particle size of each remediation material was measured using a Malvern Mastersizer 2000. The zero point of charge (if relevant) of the remediation materials in artificial soil pore water was determined using a Malvern Zetasizer.

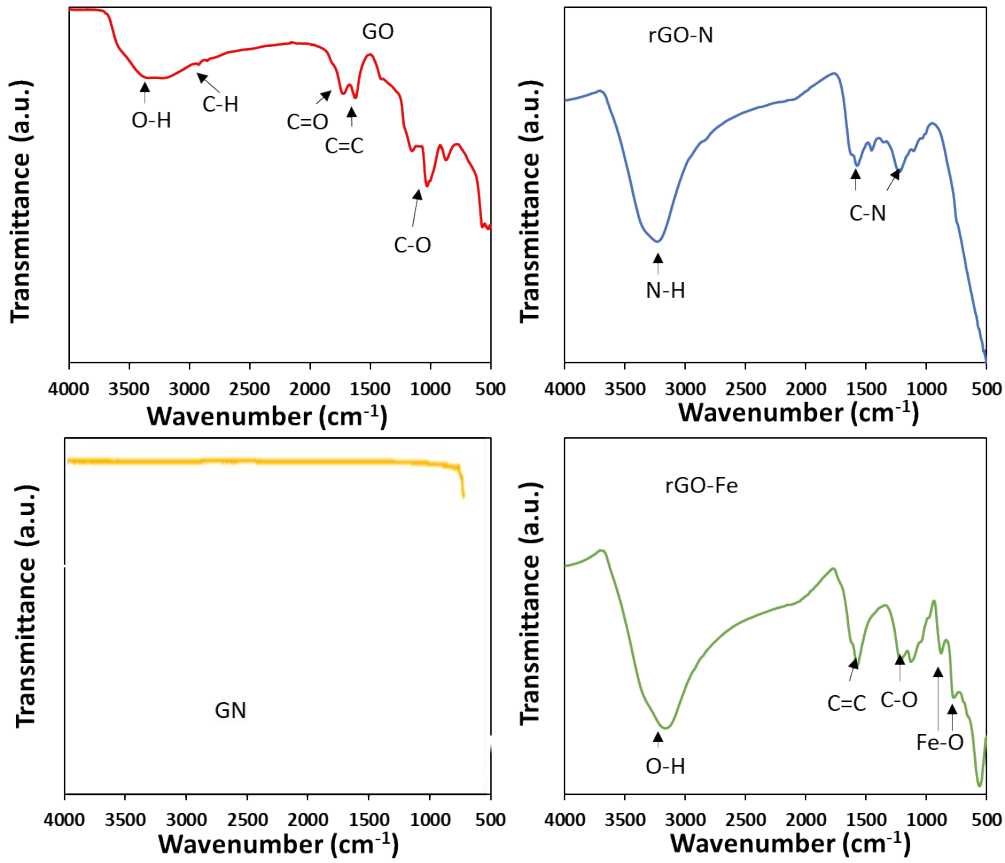

Figure S1. FTIR spectra of all synthesised graphene-based materials.

Table S2. Concentration of different PFAS in AFFF-solution. Diluted AFFF-solution was used for batch sorption experiments. (LOD, ND and NA refer to the method detection limit, not detected and not reported, respectively)

PFAS	Compound	Detected concentration (μg/L)	Selected PFAS concentration in diluted AFFF-solution (μg/L)
Perfluoroalkyl carboxylic acids (PFCAs)	PFBA	399.1	NA
	PFPeA	301	NA
	PFHxA*	2205.1	33.1±1.0
	PFHpA	591.6	NA
	PFOA	1734.9	NA
	PFDA	<LOD*	NA
	PFUdA	<LOD*	NA
	PFDoA	<LOD*	NA
	PFTrDA	<LOD*	NA
	PFTeDA	<LOD*	NA
Perfluoroalkane sulfonic acids (PFSAs)	PFBS	3088.4	NA
	PFPeS	2099.2	NA
	PFHxS*	18229	166.0±4.7
	PFHpS	1791	NA
	PFOS	530840	NA
	PFNS	558	NA
	PFDS	305	NA
Perfluoroalkyl Sulfonamides	PFOSA	25.6	NA
	N-EtFOSAA	2.1	NA
Other PFAS	N-AP-FHxSA*	4332.5	46.0±3.2
	N-CMAmP-6:2FOSA*	ND	NA
	N-TAmP-FHxSA*	4124.1	47.9±4.6

Table S3. Selected physical and chemical properties of PFAS-contaminated soil.

Salinity EC 1:5	dS/m	0.34
pH 1:5 water	pH units	7.1
Organic carbon	%	0.8
Clay	%	2.5
Sand	%	92
Silt	%	5.6
Texture		Sand

Table S4. Mean total concentrations of PFAS in soils and method detection limits of analysed PFAS (standard deviations are based on three replications).

PFAS	Concentration (µg/kg)	LOR
PFBS	12.3±0.3	0.2
PFPeS	21±0.8	0.2
PFHxS	293.3±10	0.2
PFHpS	72.7±3.5	0.2
PFOS	14633.3±585.9	0.2
PFDS	133.7±3.1	0.2
PFBA	24.2±1.6	1
PFPeA	104.3±5.1	0.2
PFHxA	27.7±1.3	0.2
PFHpA	80.5±4.2	0.2
PFOA	22.1±0.9	0.2
PFNA	14.8±0.8	0.2
PFDA	11.3±0.8	0.2
PFUnDA	7±1.3	0.2
PFDoDA	24.2±1.6	0.2
FOSA	99±9	0.2
8:2 FTS	16.3±2.5	0.5
10:2 FTS	140±8.4	0.5
N-AP-FHxSA	533±8.2	0.8
N-TAmP-FHXSA	1328.2±221	0.9
5-1-2 FtB	1386.9±1.7	0.6
N-CMAmP-6:2FOSA	1171.8±86	1.3
6:2 FTS	43.2±1.4	0.4
8:2 FTS	178.2±24	0.4

Table S5. The method detection limit (LOD)and quantification (LOQ) on the LC-MS/MS.

PFAS	LOD(µg/L)	LOQ(µg/L)
N-AP-FHxSA	0.8	2.4
N-TAmP-FHxSA	0.9	2.7
N-CMAmP-6:2FOSA	1.3	4.0
PFHxA	0.4	1.3
PFHxS	1.3	3.9

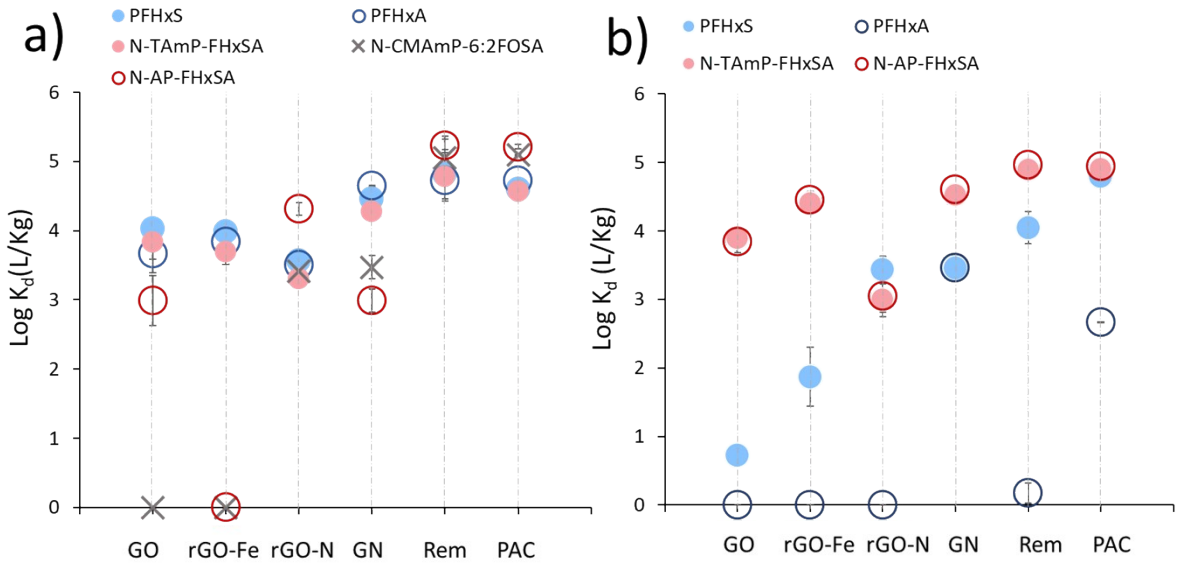

Figure S2. Partitioning of the selected anionic and zwitterionic PFAS to different GNBs, PAC and GAC using a) artificial PFAS solution and b) AFFF-spiked solution.

Calculations

PFAS sorbed is presented in terms of the K_d, the solid/liquid partition coefficient, of the PFAS onto the remediation agent, through the following equation in the units of L/kg.

$$K_d = \frac{[PFAS\ sorbed\ to\ sorptive\ materials]}{[PFAS\ remained\ in\ the\ liquid]} \qquad \text{eq.1}$$

Where, the amount of PFAS sorbed on sorptive material (µg/kg) calculated following the eq. 2

$$[PFAS\ sorbed\ to\ sorptive\ materials\ ] = \frac{([PFAS]_{Initial} - [PFAS]_{Rem})\ (\frac{\mu g}{L}) \times\ V\ (L)}{m\ (kg)} \qquad \text{eq. 2}$$

and the amount of PFAS remained in the artificial soil pore water after remediation was measured by LC-MS/MS and reported as µg/L. It should be noted that the reported K_d does not represent the equilibrium K_d values.

Each sorptive material was tested individually in artificial soil pore water for remediation ability on the artificial PFAS mixture of increasing concentrations, from 10 µg/L – 300 µg/L to attempt to pinpoint the sorption mechanism and capacity of each remediation agent. The data was fitted against two linear adsorption models, Langmuir and Freundlich (Ayawei *et al.*, 2017). The Langmuir adsorption model takes the form of the following equation (eq. 3).

$$\frac{C_e}{Q_e} = \frac{1}{Q_{max}} \times C_e + \frac{1}{Q_{max} \times K_L} \quad \text{eq.3}$$

Where, Q_e= quantity of adsorbate adsorbed by the adsorbent (mg/g), Q_{max} is the maximum amount of absorbate that the adsorbent can adsorb (mg), K_L is the Langmuir equilibrium constant, and C_e is the equilibrium concentration of the adsorbate remaining in solution (µg/L).

The Freundlich isotherm model can be found below.

$$Log(Q_e) = n\,Log(C_e) + Log\,(K_F) \quad \text{eq. 4}$$

Where, K_F is the Freundlich equilibrium constant ((µg/mg)/(µg/L)^n), and n is the fitting parameter.

The percentage immobilised referred to the percentage of the PFAS compound immobilised on the remediation material. It was calculated using the following equation.

$$\%\ immobilised = 100 - \left[\left(\frac{[PFAS]_{immobilised}}{PFAS_{unimmobilised}}\right) \times 100\right] \quad \text{eq.5}$$

Where, $[PFAS]_{immobilised}$ refers to concentration of PFAS (µg/L) in the leachates of treated soil, and $PFAS_{unimmobilised}$ refers to the concentration of PFAS (µg/L) in the untreated soil leachate.

Statistical analysis and experimental design

A range of statistical methods were implemented across the study. The batch sorption experiment was a 5 x 5 x 2 randomised block design with 3 replications. An analysis of variance (ANOVA) was performed using IBM-SPSS statistical software to obtain least significant differences (LSDs) (see Table S8a).

The experiment on the effect of pH was split into 2 x factorial design experiments, 6 remediation agents x 5 PFAS x 3 pH values for the artificial PFAS mixture, and 6 remediation agents x 4 PFAS x 3 pH values for the AFFF extract. Each set of data was analysed using IBM-SPSS statistical software to perform a multivariate ANOVA utilising LSDs of homogeneous subsets (see Table). Due to the magnitude of difference between the results for the anions (PFHxS and PFHxA) and the zwitterions for

the artificial PFAS mixture, the two subsets were split into their own ANOVA analyses. These results and further information are presented in Table S6-8.

Table S6. a) ANOVA test for between subjects' differences to determine significant differences in the mean unadjusted Log K_d in the artificial PFAS study, b) Post hoc test (multiple comparisons of homogeneous subsets) to determine LSDs for the artificial PFAS mixture and c) Post hoc test (multiple comparisons of homogeneous subsets) to determine LSDs for all data – AFFF- spiked solution.

Table S6a: ANOVA test for between subjects' differences to determine significant differences in the mean unadjusted Log K_d in the artificial PFAS study

Source	Significance
PFAS type	<0.001
pH	<0.001
sorbents	<0.001
PFAS type * pH	<0.001
PFAS type * sorbent	<0.001
pH * sorbent	<0.001
PFAS type * pH * sorbent	<0.001

Table S6b: Post hoc test (multiple comparisons of homogeneous subsets) to determine LSDs for the artificial PFAS mixture.

(I) sorbent	(J) sorbent	Sig.	(I) PFAS type	(J) PFAS type	Sig.
			N-AP-FHxSA	**N-CMAmP-6:2FOSA**	<0.001
rGO-Fe	**GN**	0.9		**N-TAmP-FHxSA**	0.383
	GO	0.9		**PFHxA**	0.633
	rGO-N	0.9		**PFHxS**	0.595
	PAC	0.002	**N-CMAmP-6:2FOSA**	**N-AP-FHxSA**	<0.001
	RemBind	<0.001		**N-TAmP-FHxSA**	<0.001
GN	**rGOFe**	0.9		**PFHxA**	<0.001
	GO	0.8		**PFHxS**	<0.001
	rGO-N	0.8	**N-TAmP-FHxSA**	**N-AP-FHxSA**	0.383
	PAC	0.004		**N-CMAmP-6:2FOSA**	<0.001
	RemBind	<0.001		**PFHxA**	0.178
GO	**rGO-Fe**	0.9		**PFHxS**	0.733
	GN	0.8	**PFHxA**	**N-AP-FHxSA**	0.633
	rGO-N	0.9		**N-CMAmP-6:2FOSA**	<0.001
	PAC	0.002		**N-TAmP-FHxSA**	0.178
	RemBind	<0.001		**PFHxS**	0.313
rGO-N	**rGO-Fe**	1	**PFHxS**	**N-AP-FHxSA**	0.595
	GN	0.8		**N-CMAmP-6:2FOSA**	<0.001
	GO	1		**N-TAmP-FHxSA**	0.733
	PAC	0.002		**PFHxA**	0.313
	RemBind	<0.001	**(I) pH**	**(J) pH**	**Sig.**
PAC	**RGO-Fe**	0.002	**4**	**6.5**	0.033
	GN	0.004		**9**	<0.001
	GO	0.002	**6.5**	**4**	0.033
	rGO-N	0.002		**9**	<0.001
	RemBind	<0.001	**9**	**4**	<0.001
RemBind	**rGO-Fe**	<0.001		**6.5**	<0.001
	GN	<0.001			
	GO	<0.001			
	rGO-N	<0.001			
	PAC	<0.001			

Table S6c: Post hoc test (multiple comparisons of homogeneous subsets) to determine LSDs for all data – AFFF- spiked solution.

(I) sorbent	(J) sorbent	Sig.
rGO-Fe	GN	0.1
	GO	0.8
	rGO-N	0.6
	PAC	<0.001
	RemBind	<0.001
GN	rGO-Fe	0.1
	GO	0.1
	rGO-N	0.03
	PAC	<0.001
	RemBind	<0.001
GO	rGO-Fe	0.8
	GN	0.06
	rGO-N	0.8
	PAC	<0.001
	RemBind	<0.001
rGO-N	rGO-Fe	0.6
	GN	0.03
	GO	0.8
	PAC	<0.001
	RemBind	<0.001
PAC	rGO-Fe	<0.001
	GN	<0.001
	GO	<0.001
	rGO-N	<0.001
	RemBind	<0.001
RemBind	rGO-Fe	<0.001
	GN	<0.001
	GO	<0.001
	rGO-N	<0.001
	PAC	<0.001

(I) PFAS type	(J) PFAS type	Sig.
N-AP-FHxSA	N-TAmP-FHxSA	<0.001
	PFHxA	<0.001
	PFHxS	<0.001
N-TAmP-FHxSA	N-AP-FHxSA	<0.001
	PFHxA	<0.001
	PFHxS	<0.001
PFHxA	N-AP-FHxSA	<0.001
	N-TAmP-FHxSA	<0.001
	PFHxS	0.007
PFHxS	N-AP-FHxSA	<0.001
	N-TAmP-FHxSA	<0.001
	PFHxA	0.007

Table S7: Post hoc test (multiple comparisons of homogeneous subsets) to determine LSDs for zwitterionic PFAS only – artificial PFAS mixture.

(I) pH	(J) pH	Sig.	(I) PFAS type	(J) PFAS type	Sig.
4	**6.5**	<0.001	**N-AP-FHxSA**	**N-CMAmP-6:2FOSA**	<0.001
	9	0.9		**N-TAmP-FHxSA**	0.5
6.5	**4**	<0.001	**N-CMAmP-6:2FOSA**	**N-AP-FHxSA**	<0.001
	9	<0.001		**N-TAmP-FHxSA**	<0.001
9	**4**	0.9	**N-TAmP-FHxSA**	**N-AP-FHxSA**	0.5
	6.5	<0.001		**N-CMAmP-6:2FOSA**	<0.001

Table S8: Post hoc test (multiple comparisons of homogeneous subsets) to determine LSDs for anionic PFAS only – artificial PFAS mixture.

(I) sorbent	(J) sorbent	Sig.	(I) pH	(J) pH	Sig.
rGO-Fe	**GN**	0.7	**4**	**6.5**	<0.001
	GO	1		**9**	0.9
	rGO-N	0.9	**6.5**	**4**	<0.001
	PAC	<0.001		**9**	<0.001
	RemBind	<0.001	**9**	**4**	0.9
GN	**rGO-Fe**	0.8		**6.5**	<0.001
	GO	0.8			
	rGO-N	0.8			
	PAC	<0.001			
	RemBind	<0.001			
GO	**rGO-Fe**	1			
	GN	0.8			
	rGO-N	0.9			
	PAC	<0.001			
	RemBind	<0.001			
rGO-N	**rGO-Fe**	0.9			
	GN	0.8			
	GO	0.9			
	PAC	<0.001			
	RemBind	<0.001			
PAC	**rGO-Fe**	<0.001			
	GN	<0.001			
	GO	<0.001			
	rGO-N	<0.001			
	RemBind	<0.001			
RemBind	**rGO-Fe**	<0.001			
	GN	<0.001			

	GO	<0.001
	rGO-N	<0.001
	PAC	<0.001

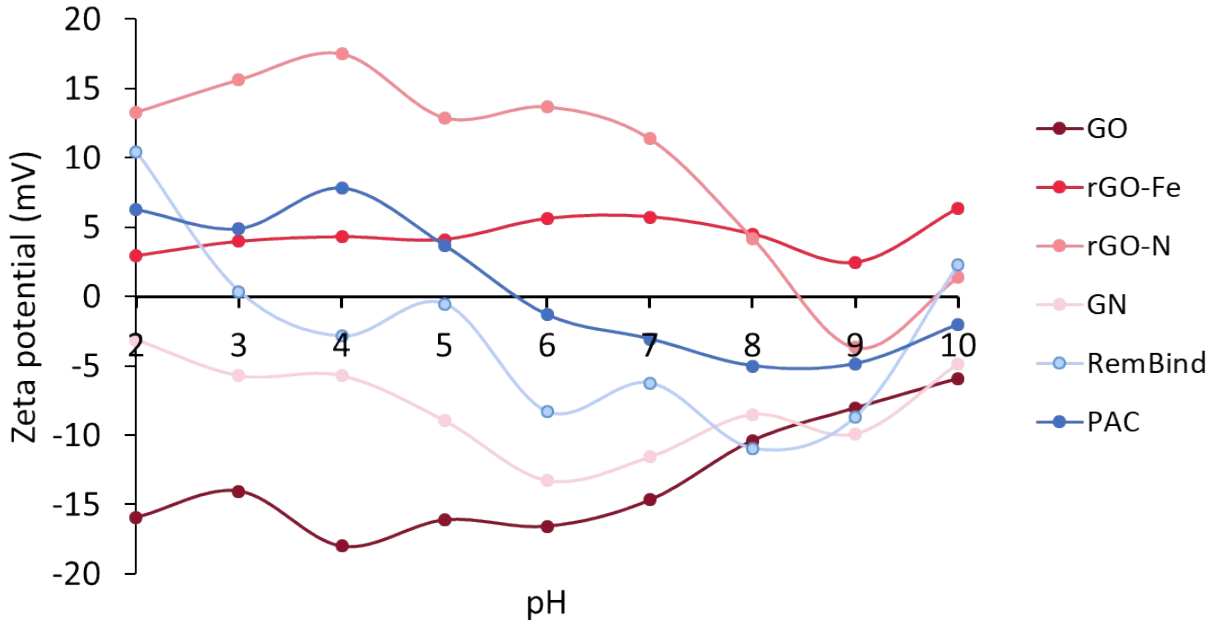

Figure S3. Zeta potential of graphene based materials, PAC and RemBind in soil pore water.

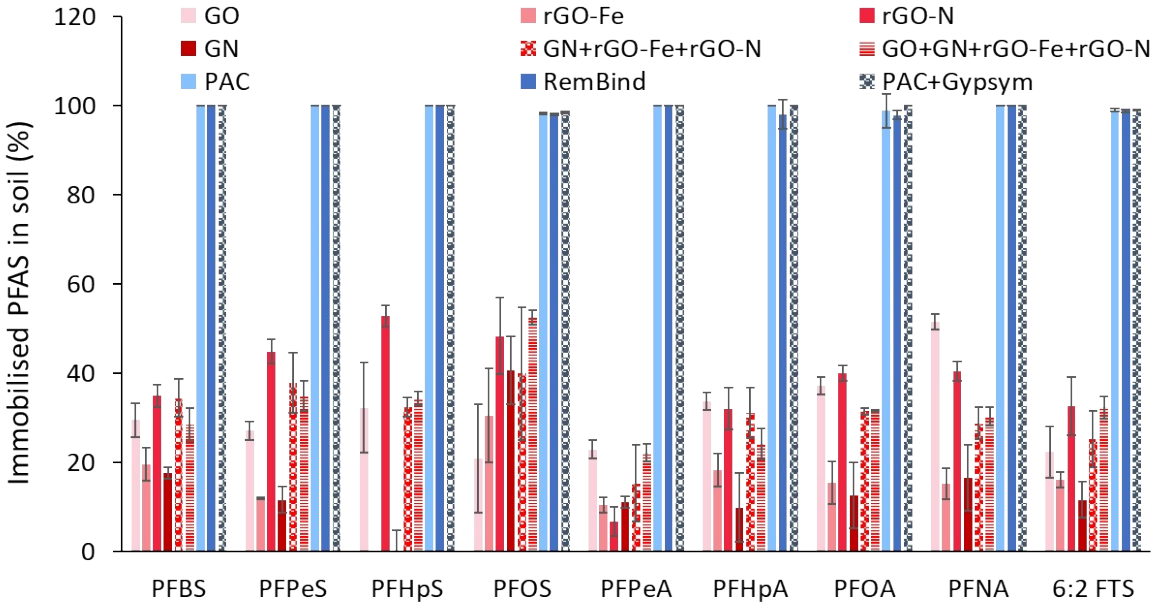

Figure S4. Percentage of immobilised PFAS in treated soil with different sorbents. Error bars are based on standard deviations of n = 3 samples.

Refrences:

Andjelkovic, I., D.N.H. Tran, S. Kabiri, S. Azari, M. Markovic and D. Losic, 2015. Graphene aerogels decorated with α-feooh nanoparticles for efficient adsorption of arsenic from contaminated waters. ACS Applied Materials & Interfaces, 7(18): 9758-9766. Available from http://dx.doi.org/10.1021/acsami.5b01624. DOI 10.1021/acsami.5b01624.

Ayawei, N., A.N. Ebelegi and D. Wankasi, 2017. Modelling and interpretation of adsorption isotherms. Journal of Chemistry, 2017: 3039817. Available from https://doi.org/10.1155/2017/3039817. DOI 10.1155/2017/3039817.

Kabiri, S., D.N.H. Tran, T. Altalhi and D. Losic, 2014. Outstanding adsorption performance of graphene–carbon nanotube aerogels for continuous oil removal. Carbon, 80: 523-533. Available from https://www.sciencedirect.com/science/article/pii/S000862231400832X. DOI https://doi.org/10.1016/j.carbon.2014.08.092.

Kabiri, S., D.N.H. Tran, R. Baird, M.J. McLaughlin and D. Losic, 2020. Revealing the dependence of graphene concentration and physicochemical properties on the crushing strength of co-granulated fertilizers by wet granulation process. Powder Technology, 360: 588-597. DOI 10.1016/j.powtec.2019.10.047.

Marcano, D.C., D.V. Kosynkin, J.M. Berlin, A. Sinitskii, Z. Sun, A. Slesarev, L.B. Alemany, W. Lu and J.M. Tour, 2010. Improved synthesis of graphene oxide. ACS Nano, 4(8): 4806-4814. Available from https://doi.org/10.1021/nn1006368. DOI 10.1021/nn1006368.

Yap, P.L., T.T. Tung, S. Kabiri, N. Matulick, D.N.H. Tran and D. Losic, 2020. Polyamine-modified reduced graphene oxide: A new and cost-effective adsorbent for efficient removal of mercury in waters. Separation and Purification Technology, 238: 116441. Available from https://www.sciencedirect.com/science/article/pii/S138358661933730X. DOI https://doi.org/10.1016/j.seppur.2019.116441.